Effect of interface bonding on spin-dependent tunneling from the oxidized Co surface

K. D. Belashchenko,[1] E. Y. Tsymbal,[1] M. van Schilfgaarde,[2] D. A. Stewart,[3] I. I. Oleynik,[4] and S. S. Jaswal[1]

[1]Department of Physics and Astronomy and Center for Materials Research and Analysis, University of Nebraska, Lincoln, Nebraska 68588

[2]Department of Chemical and Materials Engineering, Arizona State University, Tempe, Arizona 85287

[3]Sandia National Laboratories, Livermore, California 94551

[4]Department of Physics, University of South Florida, Tampa, Florida 33620

We demonstrate that the factorization of the tunneling transmission into the product of two surface transmission functions and a vacuum decay factor allows one to generalize Julliere's formula and explain the meaning of the "tunneling density of states" in some limiting cases. Using this factorization we calculate spin-dependent tunneling from clean and oxidized fcc Co surfaces through vacuum into Al using the principal-layer Green's function approach. We demonstrate that a monolayer of oxygen on the Co (111) surface creates a spin-filter effect due to the Co-O bonding which produces an additional tunneling barrier in the minority-spin channel. This changes the minority-spin dominated conductance for the clean Co surface into a majority spin dominated conductance for the oxidized Co surface.

I. INTRODUCTION

Spin-dependent tunneling (SDT) in magnetic tunnel junctions (MTJs) is a dynamically developing area of research that attracted a lot of attention due to promising applications in non-volatile random access memories and next-generation magnetic field sensors (for a recent review of SDT see Ref. 1). The experimental efforts have succeeded in achieving large reproducible tunneling magnetoresistance (TMR) in MTJs[2] but also raised fundamental questions regarding the nature of SDT. One such question is the role of the ferromagnet/insulator interfaces in controlling the spin polarization (SP) of the tunneling conductance. The SP is usually defined as $P = (G_\uparrow - G_\downarrow)/(G_\uparrow + G_\downarrow)$, where $G_\sigma = (e^2/h)\sum_{k_\parallel} T_\sigma(k_\parallel)$ is the conductance for spin channel σ, T_σ is the transmission function, and $k_\parallel$ is the lateral wave vector.

Commonly the expected spin dependence of the tunneling current is deduced by considering the symmetry of the Bloch states in the bulk ferromagnetic electrodes and the complex band structure of the insulator.[3,4] By identifying those bands in the electrodes that are allowed by symmetry to couple efficiently to the evanescent states decaying most slowly in the barrier one can predict the SP of the conductance. However, this approach has two deficiencies. First, it assumes that the barrier is sufficiently thick so that only a small focused region of the surface Brillouin zone (SBZ) contributes to the tunneling current. For realistic MTJs with a barrier thickness of about 1 nm this assumption is usually unjustified. Second, symmetry considerations alone applied to bulk materials are not always sufficient to predict the SP. It is critical to take into account the electronic structure of the ferromagnet/barrier interfaces which, as it was shown both experimentally[5] and theoretically,[6] controls SDT.

An important mechanism by which the interfaces affect the SP of the tunneling current is the bonding between the ferromagnetic electrodes and the insulator.[7] This effect was put forward to explain positive and negative values of TMR depending on the applied voltage in MTJs with Ta_2O_5 and Ta_2O_5/Al_2O_3 barriers[8] and to elucidate the inversion of the SP in $Co/SrTiO_3/La_{0.67}Sr_{0.33}MnO_3$ MTJs.[9] So far there are no theoretical studies explaining the microscopic origin of this phenomenon.

In this paper we report the results of first-principles calculations of SDT from clean and oxidized Co surfaces through vacuum into Al and demonstrate the crucial role of the bonding between Co and O atoms. This system was chosen for investigation because the MTJs based on alumina have predominantly O-terminated Co/Al_2O_3 interfaces.[10] By replacing alumina by vacuum we can ignore the complexity of the atomic structure of the amorphous alumina and focus on effects of surface oxidation. Moreover, this system can be directly studied using spin-polarized STM.[11]

We show that a monolayer of oxygen on the Co surface creates a spin-filter effect due to the Co-O bonding by producing an additional tunneling barrier in the minority-spin channel. This reverses the sign of the SP from negative for the clean Co surface to positive for the oxidized Co surface, thus revealing the crucial role of interface bonding in SDT.

II. SURFACE TRANSMISSION FUNCTIONS

We approach the tunneling problem in the spirit of perturbation theory.[12] We consider the system consisting of "left" and "right" leads separated by a relatively thick barrier and assume that two-dimensional translational periodicity in transverse directions is preserved for both electrodes including their surfaces (although it may be different for each subsystem). Every Bloch wave with a lateral quasi-wave vector $k_\parallel^L$ coming from the left lead has a decay tail in the vacuum composed of the waves with transverse wave vectors $k_\parallel^L + G_i$ where G_i are the reciprocal lattice vectors of the SBZ of the left lead.[13] At sufficient distances from the surface (typically just a

few lattice parameters for low-index surfaces) all waves with $G_i \neq 0$ vanish and may be neglected in the Fourier expansion of the Bloch wave in the vacuum. On the other hand, the quasi-wave vector k_k^R is the good quantum number for the right lead. This means that k_k is conserved across the entire system even if there is no common in-plane periodicity and k_k^L, k_k^R are defined with respect to different SBZs. In this case, each tunneling eigenstate is almost identical to an evanescent plane wave in the central region of the barrier.

For a given k_k the transmission function is the sum of the transmission coefficients for all tunneling eigenstates corresponding to all incoming Bloch waves with this k_k in the left electrode. At the same time, each transmission coefficient for a given eigenstate contains a sum over outgoing states in the right electrode with the same k_k. Let us choose a reference plane in the vacuum region at a sufficient distance from the surface of an electrode, so that the eigenstates for all k_k are already indistinguishable from the barrier eigenstates at this plane (see Fig. 1). For each tunneling eigenstate the amplitude of the barrier eigenstate between the reference planes is the only parameter coupling the left and right electrodes. Then, the S-matrix element coupling the states in the two electrodes may be written as

$$S_{pq} = S_{pr} S_{rr'} S_{r'q} \qquad (1)$$

where p is the incoming and q the outgoing Bloch states in the left and right leads respectively, r and r' denote the same vacuum eigenstate at the left and right reference planes. We omitted the dependence on k_k for all the S-matrices in Eq. (1) for brevity. The vacuum S-matrix $S_{rr'}$ simply describes the exponential decay of the wave function in the vacuum. Note that no summation is implied in (1), because the state r is uniquely defined by k_k. The simple product of S-matrices in Eq. (1) without any multiple scattering terms is a consequence of our assumption that the barrier is sufficiently thick. Thus, we see that the transmission function $T(k_k)$ of the MTJ is factorized:

$$T(k_k) = t_L(k_k) \exp\left(-2\kappa(k_k) d\right) t_R(k_k). \qquad (2)$$

Here we replaced $|S_{rr'}|^2$ by its explicit exponential form with

$$\kappa(k_k) = \left(\frac{2m\phi}{\hbar^2} + k_k^2 \right)^{1/2}, \qquad (3)$$

where ϕ is the work function, and d is the distance between the reference planes assigned to the electrodes as shown in Fig. 1. All the information about the properties of individual surfaces is described by the surface transmission functions (STF) t_L, t_R:

$$t_L(k_k) = \sum_p \left| \frac{B_r}{A_p} \right|^2, \quad t_R(k_k) = \sum_q \left| \frac{C_q}{B_{r'}} \right|^2, \qquad (4)$$

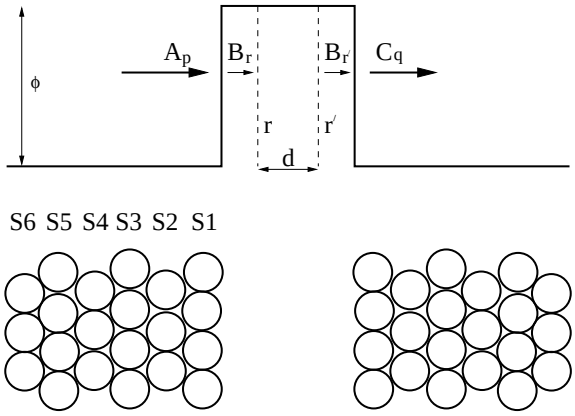

FIG. 1: Geometry of a tunnel junction with a vacuum barrier. The top graph schematically shows the potential barrier for electrons at the Fermi level. Dashed lines show the positions of the reference planes assigned to the electrodes for the calculation of the surface transmission functions. Each scattering state is described by four amplitudes: A_p of the incoming Bloch wave; B_r, B_r^0 of the surviving evanescent wave at the reference planes assigned to the left and right electrodes; and C_q of the transmitted Bloch wave in the right electrode (there may be several transmitted waves). The bottom scheme depicts atomic layers in the electrodes and their labelling used in the text.

where the four amplitudes characterize the behavior of tunneling eigenstates at the two surfaces (see Fig. 1). The different definitions of t_L and t_R are due to the fact that they obey different boundary conditions. Specifically, t_L and t_R are obtained by matching the Bloch wave functions with the vacuum eigenstates, decaying and growing into the vacuum respectively. The definition of t_L implies the solution of a scattering problem for the incoming wave with amplitude A_p, and B_r is the amplitude of this scattering eigenstate at the reference plane in the vacuum. On the other hand, t_R describes an inverse scattering problem in which the exponentially decaying wave in the vacuum with amplitude $B_{r'}$ at the reference plane is scattered on the right surface; here C_q is the amplitude of the outgoing Bloch state q in the right electrode for this "eigenstate." Note that physically, this state is forbidden because it grows to infinity in the vacuum, but it is still a formal solution of the Schrodinger equation with the specified boundary condition at infinity.

Each surface may be considered as forming the left or the right interface of the tunnel junction. It is straightforward to show that, just as in the case of a transmission matrix connecting the propagating states in the two electrodes,[14] the requirement of flux conservation results in the reciprocity condition $t_L(k_k) = t_R(k_k) \equiv t(k_k)$ for any (laterally periodic) surface, as long as the appropriate normalization of the wave functions is chosen. Specifically, all Bloch waves in the electrodes should be normalized for unit flux, while the vacuum eigenstates

should be normalized for unit "imaginary flux" $\hbar/m$. The easiest way to establish this reciprocity condition is to prove it for free electrons in a semi-infinite potential well, and then to use this free-electron system as a second electrode in a junction. Since the total transmission function for a two-electrode system is reciprocal,[14] this proves the above reciprocity condition for the STF. Note that this proof does not rely on time reversal symmetry, because time reversal also replaces k_k by $-k_k$. However, this symmetry gives another useful relation, $t(k_k;H) = t(-k_k;H)$ where H is the external magnetic field.

It is easy to see from Eq. (4) with the chosen unit flux normalization that the STF is proportional to the Fermi-level value of the k_k- and energy-resolved charge density for the given spin, which is generated by the incoming Bloch states and taken at the reference plane (any localized surface states are excluded). Indeed, the energy-resolved charge density may be written as

$$(r;E) = \frac{1}{N_k}\sum_{k_k} (r;k_k;E) \qquad (5)$$

where the k_k- and energy-resolved charge density is

$$(r;k_k;E) = \sum_p \left| F_{k_k p}(r) \right|^2 \qquad (6)$$

where the summation is over the incoming Bloch states with the given k_k and E, and the superscript F emphasizes that the scattering eigenstates $^F_{k_k p}$ are normalized so that the incoming Bloch waves carry unit flux normal to the interface. Setting $A_p = 1$ in Eq. (4), we see that $t(k_k)$ is given by Eq. (6) where r is taken at the reference plane (since we neglect all components with $G_i \neq 0$ at the reference plane, $(r;k_k;E)$ does not depend on r_k, the location within this plane).

Although we considered a vacuum tunneling barrier, the analysis can be extended to other physically important cases of insulating barriers. Indeed, the main requirement for the validity of Eqs. (1,2) is that the complex band structure be predominantly represented by a single evanescent wave for each k_k. At a minimum, this premise must hold for the "active" regions of the SBZ that contribute appreciably to the tunneling current. This means that other tunneling states must have a notably larger imaginary part of the wave vector compared to the dominant one. In the case of a vacuum barrier, this amounts to the neglect of all vacuum eigenstates with $G_i \neq 0$. In practice this criterion is well satisfied for sufficiently thick wide-gap tunnel barriers, such as sp-bonded oxides. However, for any particular barrier, this assumption has to be carefully verified by checking the complex band structure of the barrier for the presence of additional slowly decaying states in the active regions of the SBZ. It is important to note that the area of the active region quickly shrinks as the barrier thickness is increased,[4] indicating that the single evanescent state criterion will often lead to an additional requirement of "sufficient thickness" of the barrier. Note that this requirement is not related to a similar one stemming from the neglect of back-scattering.

The factorization (2) allows us to study tunneling between completely different electrodes. For practical purposes, the STF can be calculated using $T(k_k)$ obtained for a symmetric MTJ by factoring out the vacuum decay factor for the given choice of reference planes, and then taking the square root. The resulting STFs for different surfaces may then be convolved with an appropriate vacuum decay factor, $\exp(-2\kappa d)$, to obtain the transmission functions for asymmetric MTJs. In particular, $T(k_k)$ for the antiparallel (AP) magnetization of the two electrodes (and the TMR) can be found from the up- and down-spin STFs calculated from the transmission function for the parallel (P) magnetization.

III. GENERALIZATION OF JULLIERE'S FORMULA

Tunneling magnetoresistance is often discussed in terms of Julliere's formula[15]

$$\mathrm{TMR} = \frac{2P_L P_R}{1 - P_L P_R} \qquad (7)$$

where P_L, P_R are the "spin polarizations" of the left and right electrodes. Eq. (7) is derived from the empirical expression $G \propto {}_L {}_R$, where ${}_L$, ${}_R$ are the "tunneling densities of states" of the electrodes, and the spin polarization is defined as $P = (\uparrow - \downarrow)/(\uparrow + \downarrow)$. The popularity of this formula is due to the fact that it usually agrees reasonably well with experiment if the spin polarizations, which are directly related to the "tunneling densities of states," are taken from Meservey-Tedrow experiments[16] with the same barrier. However, the validity of Julliere's formula has been debated for a long time, and the reasons for its apparent agreement with experiment are unclear. The physical meaning of the "tunneling density of states" is also unclear, but it is obvious both from elementary quantum mechanics and from experiments that the tunneling properties of a magnetic heterostructure are determined not by the ferromagnet alone, but rather by the ferromagnet/barrier combination and by the structure of the interface. A number of explicit first-principles calculations for idealized MTJs without disorder (see, e.g., Ref. 17) confirmed this fact. However, it was suggested[18] that phase decoherence due to disorder which is always present in realistic MTJs may recover the factorization of the tunneling conductance in a product of "transport densities of states," which are essentially equal to the regular densities of states at the surfaces of the electrodes if there are no resonant localized states in the barrier. Moreover, it was shown[19] within a single-band tight binding model that in the limit of strong disorder one recovers Julliere's formula (7) by identifying P_L, P_R with the measurable spin polarizations of the

tunneling current for the same electrode/barrier systems. Therefore, it seems that there are good reasons for the widespread use of Julliere's formula, and it is highly desirable to elucidate these reasons.

Let us explore the connection between Eq. (2) and Julliere's formula (7). In Eq. (2) the simple product of the "tunneling densities of states" is replaced by a convolution of STFs, which explicitly include the effects of bulk densities of states and of the surface structure. Thus we can consider Eq. (2) as a generalization of Julliere's formula for an ideal MTJ with no disorder.

However, we may go further and identify limiting cases where Eq. (2) can be directly related to Julliere's formula, providing formal definitions of the "tunneling densities of states" of the electrodes appropriate for these cases. First, consider the case of a disordered insulating barrier. Such a barrier may be characterized by its eigenstates, half of which are decaying from left to right, and the other half from right to left. Although these eigenstates do not have a conserved k_k any more, it is still clear that tunneling will be dominated by Feynman paths that do not "loop back," because each path carries a weight decaying exponentially with its length (see below). Therefore, we may still write an expression similar to Eq. (1) neglecting back-scattering, but now we should sum up over all barrier eigenstates (now defined in real space). Within this formulation $S_{rr'}$ is still diagonal because it describes the decay of a single eigenstate.

The weight of a Feynman path in the imaginary-time functional integral often used for tunneling problems[20] (with Euclidean action written in its reduced Minkowskii form; see, e.g., Ref. 21) is given by $\exp\left(-\int \kappa(l)\,dl\right)$ up to a prefactor, where the integral is taken along the path, $\kappa = [2m(V-E)]^{1/2}$ and $V(r)$ is the potential. In an ordered insulator many paths with similar weights contribute to the path integral resulting in the formation of the complex band structure. However, in a disordered insulator the tunneling current may be dominated by Feynman paths running close to a relatively small number of "easy" paths with locally maximum weights, i.e. by imaginary-time classical paths.[20,21] If there is only one such channel or one class of channels with similar properties (e.g., due to surface roughness), Eq. (2) will produce Julliere's formula where P is simply the Fermi-level value of the energy-resolved charge density given by Eq. (6) integrated over k_k and taken at some reference point within the channel. (Now each term describes the scattering eigenstate corresponding to the single incoming Bloch wave with the given k_k.) Like STF, this quantity does not depend on the properties of the other side of the barrier. This conclusion agrees with the results of Ref. 19 showing that the tunneling current through a strongly disordered barrier is dominated by a small number of random configurations, and that Julliere's formula is also recovered in this limit.

Now consider the case when disorder is weak close to the interfaces, but remains strong in the insulator. Obviously, the S-matrix of the disordered insulator in k_k representation will be essentially a random matrix, and after averaging Eq. (2) thus yields Julliere's formula with $P \propto \sum_{k_k} t(k_k)$. This case is the easiest from the computational point of view, because the STFs may be directly calculated for a k_k-conserving MTJ.

It is instructive to compare this result with the conclusions of Mathon and Umerski[18] on the applicability of Julliere's formula obtained using the transfer Hamiltonian formalism. Our approach shares in common with Ref. 18 the neglect of multiple reflections across the junction. However, the assumption of constant matrix elements (hopping integrals) for all Bloch waves made in Ref. 18 completely removes all physical effects connected with orbital- and spin-dependent bonding at interfaces. This obviously contradicts the experimental findings showing that the spin polarization of the tunneling current and magnetoresistance strongly depend on the type of barrier used.[1] In our approach, the STFs for the electrodes allow us to encapsulate the effects of the interface structure and provide the proper dependence of the tunneling current on barrier type. Julliere's formula obtained in the limiting case of full decoherence inside the insulator is expressed in terms of the spin polarization actually measured in the Meservey-Tedrow experiment (assuming that the superconductor acts as an ideal, non-biased spin detector).

Finally, for very thick k_k-conserving barriers the tunneling current may be carried predominantly by a close vicinity of some special k_k-points in the SBZ (e.g., the $\bar{\Gamma}$ point). In this case, the tunneling density of states is simply equal to the value of $T(k_k)$ at this k_k.

It is not clear a priori whether any one of these three limiting cases is directly applicable to realistic MTJs, although it seems that disorder in the insulator together with the "channelization" of the tunneling current are both likely to play a major role. However, the emergence of Julliere's formula in these different scenarios suggests that it may actually have a rather wide range of applicability. In general, the "tunneling density of states" should be identified with some appropriately averaged energy-resolved charge density taken at the Fermi level at a sufficient distance from the interface within the barrier. Unlike the bulk density of states, this function fully takes into account the relevant properties of the surface.

IV. TUNNELING FROM CLEAN AND OXIDIZED Co(111) SURFACES THROUGH VACUUM INTO Al

We calculated the transmission functions using the principal-layer Green's function approach[22] based on the tight-binding linear muffin-tin orbital method (TB-LMTO) in the atomic sphere approximation (ASA) and the transmission matrix formulation of Ref. 23. All the atomic potentials were determined self-consistently within the supercell approach using the TB-LMTO-ASA method. The vacuum barrier was modeled using empty

spheres in the positions corresponding to the continuation of the crystal lattice of the electrodes. We have also performed full-potential LMTO calculations[24] which confirmed all main features of the band structure of the oxidized Co (111) surface discussed below.

We checked the validity of factorization (2) by calculating $T(k_k)$ for (100) and (111)-oriented fcc Co electrodes with parallel magnetizations, taking the square root, and convolving $t_\uparrow(k_k)$ with $t_\downarrow(k_k)$. Then, the result was compared with the independent calculation for the antiparallel configuration in a range of energies. The agreement was always excellent (better than 1%), except for a couple of specific energies for a (100) MTJ with four vacuum "monolayers" where narrow resonances appear in the minority channel.[25] If the vacuum barrier is extended to 8 monolayers, excellent agreement is restored.

Using the factorization (2) we investigated the SP of the conductance from ferromagnetic electrodes to a nonmagnetic material, Al (111), which served as a detector of the tunneling SP in the spirit of the Meservey-Tedrow experiments.[16] As expected, the calculated STF of Al is free-electron-like, having almost perfect Gaussian shape originating from the vacuum decay factor up to the reference plane. Therefore, this surface may be considered as equally transparent for all Bloch waves, and the total transmission function for a MTJ with Al spin-detector electrode is essentially a product of the other electrode's STF and the vacuum decay factor.

First, we discuss the properties of a Co/vacuum/Al MTJ with a clean Co (111) surface. Figs. 2a,b show the k_k-resolved transmission for the majority- and minority-spin electrons within the SBZ of Co (111). The Fermi surface of Co viewed along the [111] direction has holes close to the point with no bulk states in both spin channels, which results in zero conductance in this area. The majority-spin transmission (Fig. 2a) varies rather smoothly and is appreciable over a relatively large area of the SBZ. On the other hand, the minority-spin transmission (Fig. 2b) has a narrow crown-shaped "hot ring" around the edge of the Fermi surface hole. The analysis of layer and k_k-resolved density of states (DOS) shows that it is not associated with surface states,[25] but rather with an enhancement of bulk k_k-resolved DOS near the Fermi surface edge (compare Fig. 2b with Fig. 4c).

As seen from Figs. 2a,b, the Fermi surface hole is smaller for majority spins. Therefore, the conductance should become fully majority-spin polarized in the limit of very thick barriers. However, since the Fermi surface hole is also quite narrow for minority spins, positive SP is only achieved at very large barrier thicknesses $d \gtrsim 10$ nm, while for typical values of $d \sim 2$ nm the SP is about 60% and depends weakly on d.

The oxidized Co surface was modeled by an O monolayer placed on top of the Co(111) electrode. The equilibrium atomic structure of this surface was found using the pseudopotential plane-wave method[26] within the generalized gradient approximation. We used both types of stacking: ABCA and ABCB, where the last symbol designates the position of the O monolayer. The O atoms are assumed to lie in symmetric positions above the second (S2) or first (S1) sub-surface Co layer, respectively (these layers are shown in Fig. 1 in the absence of the O monolayer). We allowed the O layer and two Co layers (S1 and S2) to relax in the direction normal to the surface, while the positions of atoms in deeper layers (S3,...) were kept fixed. The energies of both equilibrium configurations of oxygen monolayers were found to be very close to each other. All results of interest in the present context are quite similar for these two stackings. Below all specific data are given for the ABCB stacking. The equilibrium interlayer distances were found to be 2.14 Å between layers S3 and S2, 2.18 Å between S2 and S1, and 1.08 Å between S1 and O layers, compared to 2.07 Å between the adjacent Co layers in the bulk. The Co-O bond length is equal to 1.82 Å.

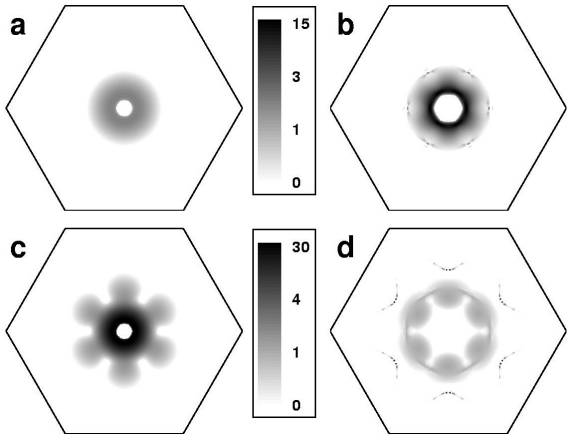

FIG. 2: k_k-resolved transmission (logarithmic scale) from clean and oxidized (111) Co surfaces through vacuum into Al. (a) Clean surface, majority spin. (b) Clean surface, minority spin. (c) Oxidized surface, majority spin. (d) Oxidized surface, minority spin. The vacuum layer thickness is 2 nm for clean and 1.7 nm for oxidized Co surface. The first surface Brillouin zone is shown. Units are 10^{-11} for (a), (b) and 10^{-14} for (c), (d).

Presence of oxygen at the surface of cobalt raises the question of whether electron correlations similar to those characteristic for transition-metal oxides may be strong enough to induce significant changes in the band structure at the oxidized Co surface. However, the enhancement of correlations in oxides is due to much weaker screening of Coulomb interaction compared to the metallic state. On the other hand, cobalt atoms below the oxygen monolayer preserve the close-packed configuration of bulk cobalt except for the top three nearest neighbors being absent out of twelve. Therefore, it is reasonable to expect that screening of Coulomb interaction in the 3d shell is not much weaker compared to the bulk. For this reason, we believe that LDA electronic structure of the oxidized Co surface is correct as far as the main features are concerned.

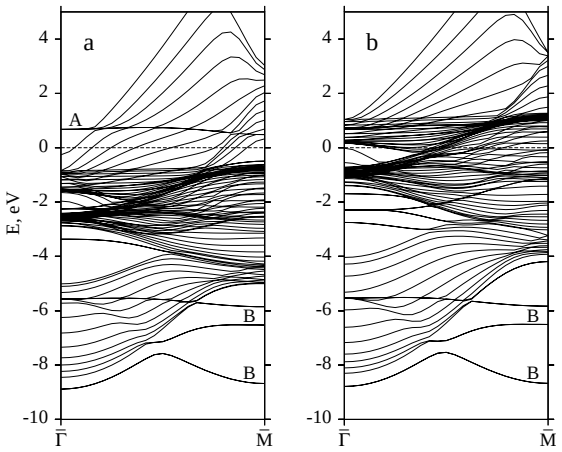

FIG. 3: Band dispersions along the $\bar{M}$ direction for (a) majority and (b) minority spin electrons. Energy is referenced from E_F. The bonding Co-O surface bands are marked B, and the pure antibonding surface band is marked A.

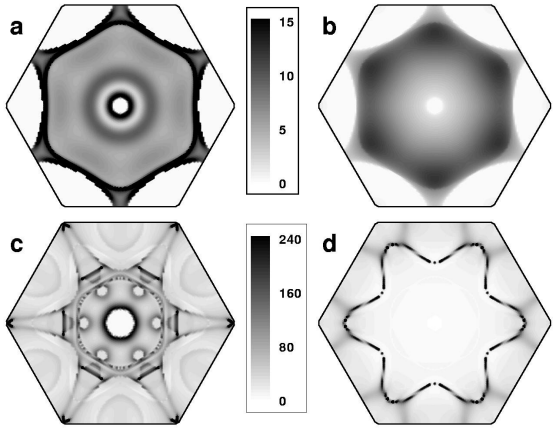

FIG. 4: k_k-resolved local DOS at E_F (arbitrary units) for the oxidized Co surface: (a) S6 layer, majority spin; (b) S1 layer, majority spin; (c) S6 layer, minority spin; (d) S1 layer, minority spin.

The oxygen monolayer dramatically changes the electronic structure of the underlying Co layer making this layer almost magnetically-dead. This change can be understood from band dispersion plots shown in Fig. 3. For each spin, the free-standing oxygen monolayer has three energy bands deriving from 2p states, each doubly degenerate due to $_z$ reflection symmetry (z is the axis normal to the surface). When the monolayer is deposited onto the Co surface, the degeneracy is lifted, and two sets of three bands each are formed corresponding to bonding and antibonding mixing of oxygen and cobalt orbitals. The three bonding bands (marked B in Fig. 3) lie well below the bulk Co 3d band, whereas the antibonding states are close to the Fermi energy E_F. As a result of this bonding the local DOS for the S1 layer at E_F is strongly reduced, so that, according to the Stoner criterion, magnetism in this layer is almost completely suppressed. The magnetic moment of Co atoms in the S1 layer is only 0.17 $_B$.

Transmission of propagating bulk states from the electrode through the barrier is very sensitive to the degree of mixing of these states with the antibonding surface states. This mixing is controlled by a selection rule which follows from the fact that all bands can be classified as "even" or "odd" according to their symmetry with respect to M reflection (M is the projection of a reflection plane). Although this classification is exact only along the $\bar{M}$ direction, it is approximately valid throughout the entire SBZ.

According to this classification, two of the three surface bands are even, and one is odd. On the other hand, the free-electron-like band of bulk Co which forms the only Fermi surface sheet for majority-spin electrons is even, while the minority-spin states on the Fermi surface sheet closest to the $\bar{\Gamma}$ point are odd. Even and odd bands are orthogonal and can not mix.

This selection rule results in the principal difference between the majority- and minority-spin transmission. The majority-spin bands are shown in Fig. 3a. One even and one odd antibonding surface bands (marked A) are degenerate at the $\bar{\Gamma}$ point (at about 0.8 eV above E_F). At a short distance from the $\bar{\Gamma}$ point both bands enter the continuum of bulk states. The odd band does not mix with the bulk states along the $\bar{M}$ line and remains almost flat due to repulsion from a lower-lying band. On the other hand, the even band readily mixes with the free-electron-like majority-spin band crossing the Fermi level and completely loses its surface localization. This is evident from Figs. 4a,b which show the k_k-resolved DOS of majority-spin electrons for the bulk-like S6 and surface S1 Co layers. The DOS for the S1 layer (Fig. 4b) is appreciable in the entire area of the SBZ where bulk states are available and has no sharp features that might indicate localized surface states. This implies that the bulk majority-spin states extend to the very surface of the electrode and therefore can readily tunnel through the barrier.

The situation is very different for minority-spin states. Although the odd surface band is again almost flat and lies above E_F, the even surface band crossing the Fermi level does not mix with the odd minority-spin band. As a consequence, the k_k-resolved DOS for Co(S1) layer (Fig. 4d) is large only along the curve lying at the periphery of the SBZ where the Co-O antibonding surface band crosses the Fermi level (oxygen DOS looks very similar). As a result, the bulk minority-spin states responsible for most tunneling transmission from the clean surface only extend up to the S2 layer, encountering a band gap in the S1 and oxygen layers. Thus, an additional tunneling barrier is introduced in the minority-spin channel, and the total SP of the tunneling transmission becomes almost 100% positive, which is evident from Figs. 2c,d.

The predicted effect of interface bonding is not limited

only to the Co(111) surface. We have also calculated the transmission from clean and oxidized Co(100) and Ni(111) electrodes and found that surface oxidation reverses the SP due to the bonding between Co or Ni with O. As it was shown earlier, the reversal of the SP also occurs for the Fe(100) surface.[27]

V. CONCLUSION

We have shown that the problem of calculating of the transmission function for a sufficiently thick insulating barrier is reduced to the solution of three separate problems, namely the penetration of the bulk wave functions into the barrier from both sides, and the behavior of the evanescent barrier eigenstates. This separation provides a natural generalization of Julliere's formula. We identified three limiting cases when the original Julliere's formula is recovered. The "tunneling density of states" in this formula is identified with an appropriately averaged energy-resolved charge density generated by the bulk Bloch states within the barrier and taken at the Fermi level.

Using the factorization of the transmission function into a product of surface transmission functions and a barrier decay factor we calculated the spin polarization of the tunneling current from clean and oxidized Co(111) surfaces through vacuum into Al. We showed that the bonding between Co and O atoms at the oxidized surface controls SDT by creating an additional barrier for minority-spin electrons, which results in a reversal of the spin polarization.

Experimentally, the reversal of the SP associated with surface oxidation may be detected using spin-polarized STM measurements.[11] Since the ferromagnetic tip is sensitive to the SP of the total local DOS above the surface (see, e.g., Ref. 28), the TMR in the system surface/vacuum/tip should change sign when the Co surface is oxidized. In other words, for the clean Co(111) surface the tunneling current should be higher when the magnetizations of the tip and the surface are aligned parallel (the dominating minority channel is then open), but for the oxidized surface it should be higher for the antiparallel configuration.

Acknowledgments

We are grateful to V. P. Antropov for useful discussions. This work is supported by NSF (DMR-0203359 and MRSEC DMR-0213808) and the Nebraska Research Initiative. MvS was supported by DARPA and ONR. Work at Sandia National Laboratories is supported by U.S. Department of Energy under contract No. DE-AC04-94AL85000.

[1] E. Y. Tsymbal, O. N. Mryasov and P. R. LeClair, J. Phys.: Condens. Matter 15, R109 (2003).
[2] J. S. Moodera, L. R. Kinder, T. M. Wong and R. Meservey, Phys. Rev. Lett. 74, 3273 (1995).
[3] J. M. MacLaren, X.-G. Zhang, W. H. Butler and X. Wang, Phys. Rev. B 59, 5470 (1999).
[4] Ph. Mavropoulos, N. Papanikolaou and P. H. Dederichs, Phys. Rev. Lett. 85, 1088 (2000).
[5] P. LeClair, H. J. M. Swagten, J. T. Kohlhepp, R. J. M. van de Veerdonk and W. J. M. de Jonge, Phys. Rev. Lett. 84, 2933 (2000); P. LeClair, J. T. Kohlhepp, H. J. M. Swagten and W. J. M. de Jonge, Phys. Rev. Lett. 86, 1066 (2001).
[6] C. Uiberacker and P. M. Levy, Phys. Rev. B 65, 169904 (2002).
[7] E. Y. Tsymbal and D. G. Pettifor, J. Phys.: Condens. Matter 9, L411 (1997).
[8] M. Sharma, S. X. Wang, and J. H. Nickel, Phys. Rev. Lett. 82, 616 (1999).
[9] J. M. De Teresa, A. Barthelemy, A. Fert, J. P. Contour, R. Lyonnet, F. Montaigne, P. Seneor and A. Vaures, Phys. Rev. Lett. 82, 4288 (1999); A. Barthelemy, A. Fert, J. P. Contour, F. Montaigne and P. Seneor, Science 286, 507 (1999).
[10] I. I. Oleinik, E. Y. Tsymbal and D. G. Pettifor, Phys. Rev. B 62, 3952 (2000).
[11] M. Bode, Rep. Prog. Phys. 66, 523 (2003).
[12] W. A. Harrison, Solid State Theory (McGraw-Hill, New York, 1970).
[13] I. I. Mazin, Europhys. Lett. 55, 404 (2001).
[14] S. Datta, Electronic transport in mesoscopic systems, (Cambridge University Press, Cambridge, UK, 1999).
[15] M. Julliere, Phys. Lett. A 54, 225 (1975).
[16] R. Meservey and P. M. Tedrow, Phys. Rep. 238, 173 (1994).
[17] J. M. MacLaren, X.-G. Zhang and W. H. Butler, Phys. Rev. B 56, 11827 (1997).
[18] J. Mathon and A. Umerski, Phys. Rev. B 60, 1117 (1999).
[19] E. Y. Tsymbal and D. G. Pettifor, Phys. Rev. B 58, 432 (1998).
[20] S. Coleman, Aspects of Symmetry, (Cambridge University Press, Cambridge, UK, 1985).
[21] M. I. Katsnelson, M. van Schilfgaarde, V. P. Antropov and B. N. Harmon, Phys. Rev. A 54, 4802 (1996).
[22] I. Turek, V. Drchal, J. Kudrnovsky, M. Sob and P. Weinberger, Electronic structure of disordered alloys, surfaces and interfaces (Kluwer, Boston, 1997).
[23] J. Kudrnovsky, V. Drchal, C. Blaas, P. Weinberger, I. Turek and P. Bruno, Phys. Rev. B 62, 15084 (2000).
[24] M. Methfessel, M. van Schilfgaarde and R. A. Casali, in: Electronic Structure and Physical Properties of Solids: The Uses of the LMTO Method, Lecture Notes in Physics, Vol. 535, ed. H. Dreysse (Springer-Verlag, Berlin, 2000).
[25] O. Wunnicke, N. Papanikolaou, R. Zeller, P. H. Dederichs, V. Drchal and J. Kudrnovsky, Phys. Rev. B 65, 064425 (2002).
[26] M. C. Payne, M. P. Teter, D. C. Allan, T. A. Arias and J. D. Joannopoulos, Rev. Mod. Phys. 64, 1045 (1992).
[27] E. Y. Tsymbal, I. I. Oleinik and D. G. Pettifor, J. Appl.

Phys. 87, 5230 (2000). Note that in this paper the SP was deduced from the local DOS in the vacuum without calculating the transmission function.

[28] S. Heinze, S. Blugel, R. Pascal, M. Bode and R. Wiesendanger, Phys. Rev. B 58, 16432 (1998).